Supplementary material for: Investigating the sign of stratocumulus adjustments to aerosols in the global storm-resolving model ICON

Emilie Fons[1], Ann Kristin Naumann[2,3], David Neubauer[1], Theresa Lang[2,3], and Ulrike Lohmann[1]

[1]Institute for Atmospheric and Climate Science, ETH Zürich, Zürich, Switzerland

[2]Max Planck Institute for Meteorology, Hamburg, Germany

[3]Meteorological Institute, Center for Earth System Research and Sustainability (CEN), Universität Hamburg, Hamburg, Germany

Correspondence: Emilie Fons (emilie.fons@env.ethz.ch)
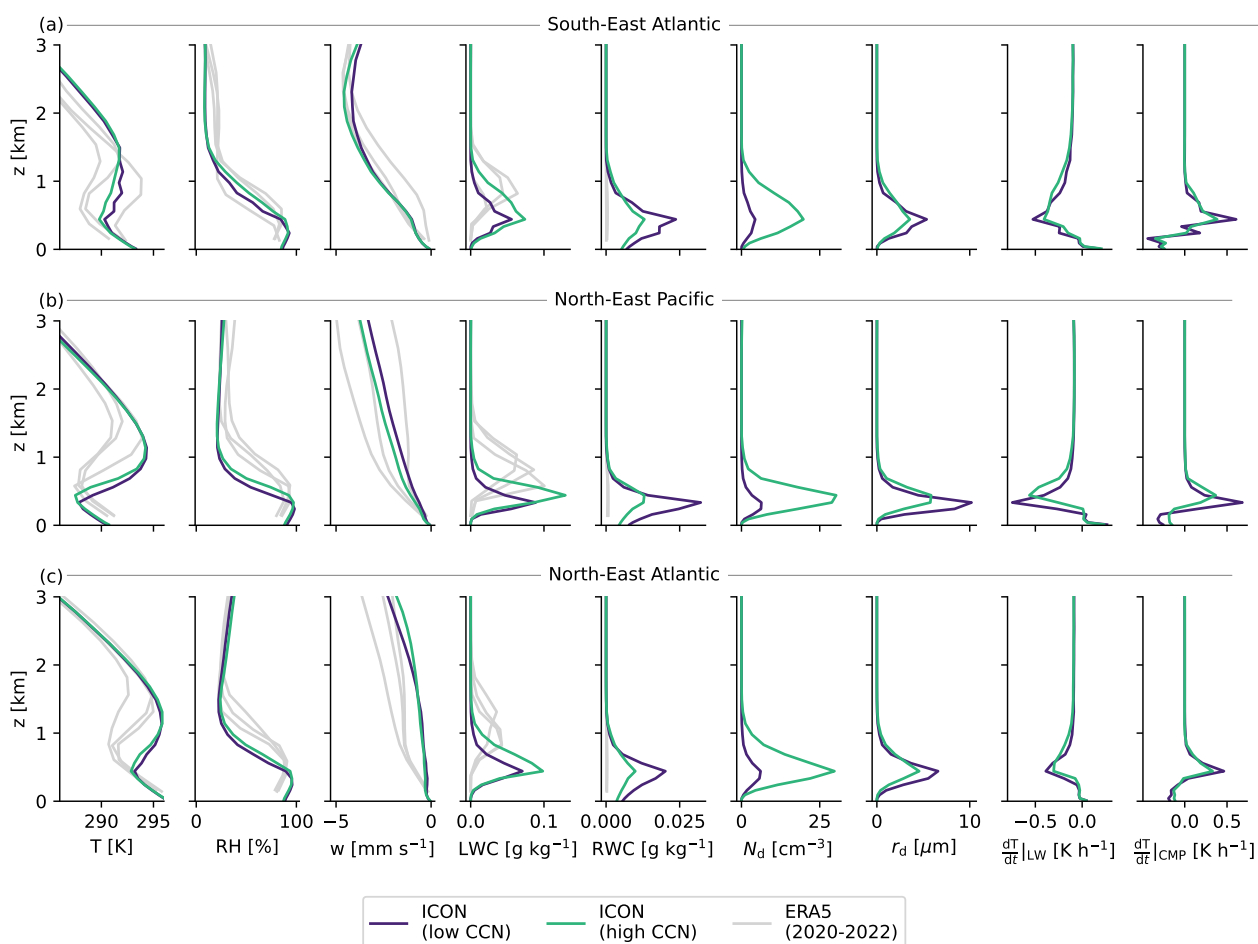
Supplementary Figure 1. Same vertical profiles as Fig. 4 and 6 but for the SEA **(a)**, NEP **(b)** and NEA **(c)** regions.
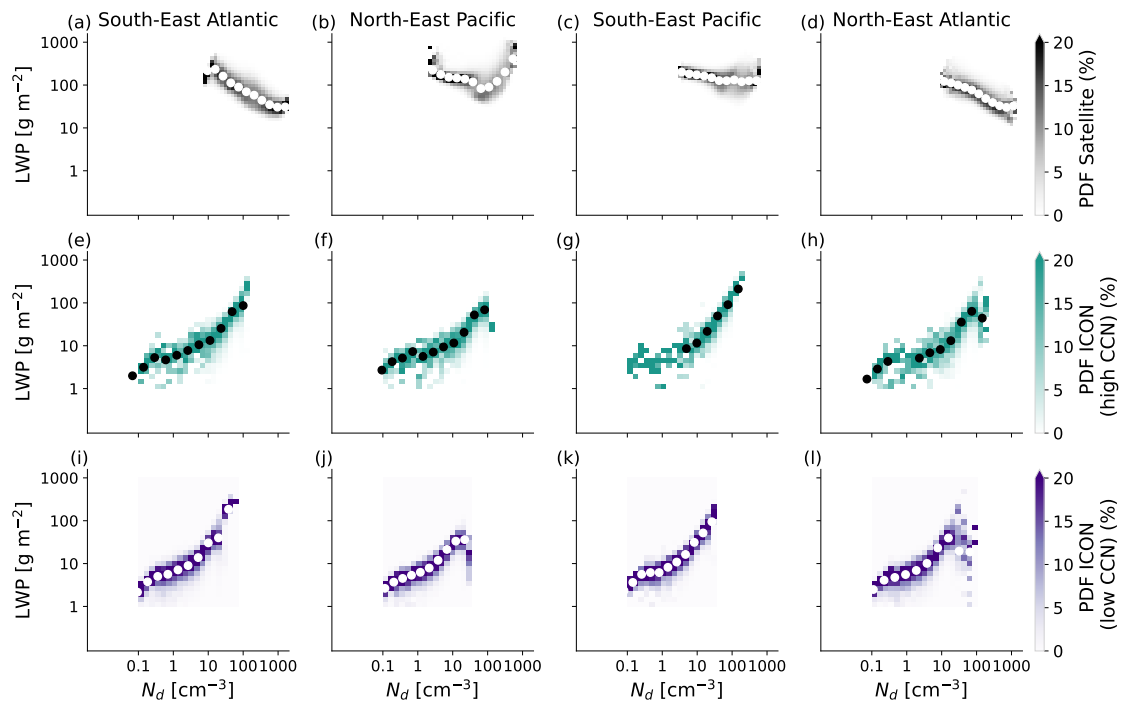
Supplementary Figure 2. Same 2D LWP vs. N_d histograms as Fig. 5, but disaggregated by region. Subplots show the regional relationships, in the satellite data **(a-d)**, the high CCN ICON experiment **(e-h)** and the low CCN ICON experiment **(i-l)**.
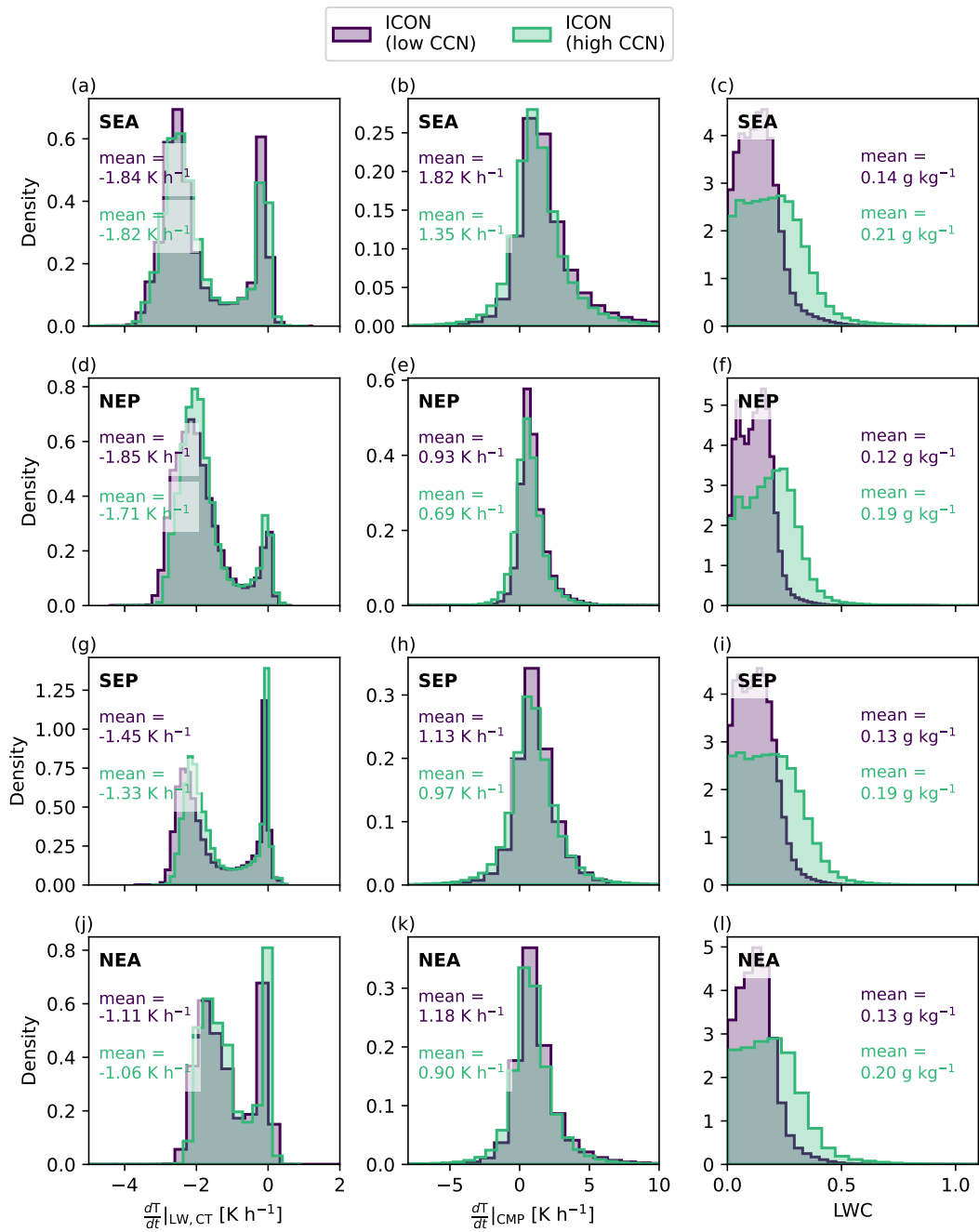
Supplementary Figure 3. Histograms of instantaneous cloud properties for the low and high CCN ICON experiments. **(a)** shows the the temperature tendencies due to longwave radiation for grid cells at cloud top for the SEA region; **(b)** shows the temperature tendencies due to the cloud microphysics scheme for SEA; **(c)** shows the liquid water content averaged over the cloud depth for SEA. **(d-f)** show the same three variables for the NEP region, **(g-i)** for the SEP region, and **(j-l)** for the NEA region.
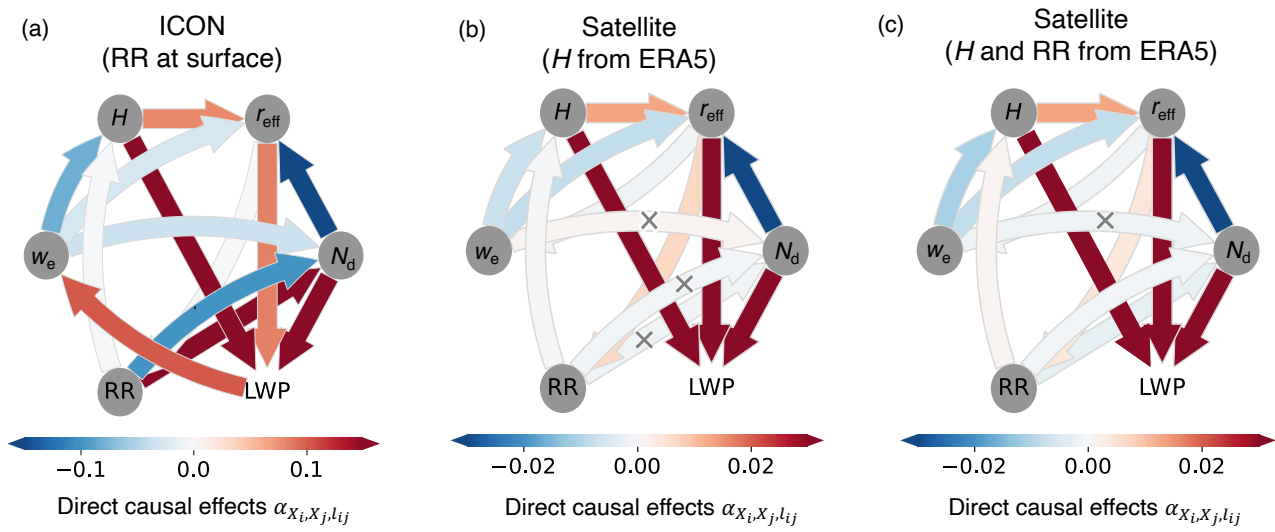
Supplementary Figure 4. Same as Fig. 7b with different proxies for H and RR. **(a)** H is estimated from the satellite data, **(b)** H is estimated from ERA5, **(c)** both H and RR are taken from ERA5.
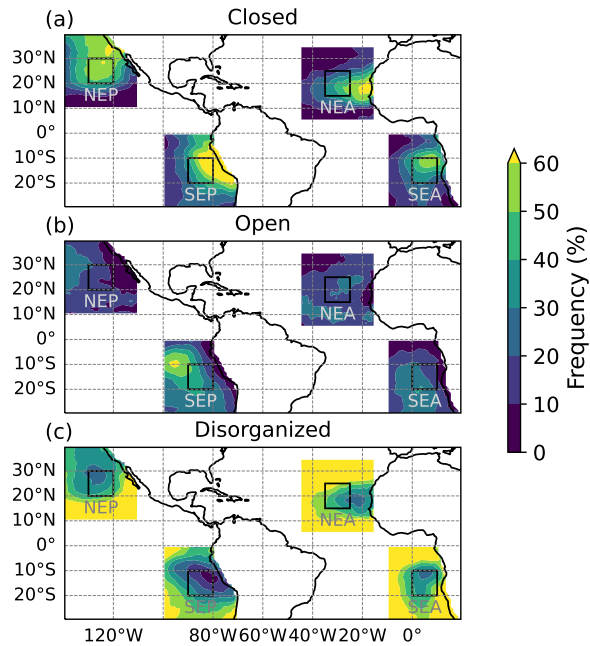
Supplementary Figure 5. Frequencies of stratocumulus morphologies, computed using the MIDAS satellite product from McCoy et al. (2023); Eastman et al. (2023). **(a)** shows the frequency of the closed-cell morphology, **(b)** shows the frequency of the open-cell morphology and **(c)** shows the frequency of the disorganized morphology. Frequencies are calculated with respect to the total number of pixels identified as one of the three morphologies in a given pixel over the time period of the data set (2003 to 2018). For each year, only the 1th of July to the 9th of August are selected to match the time period of this study. Maps from cartopy (Met Office, 2010 - 2015)
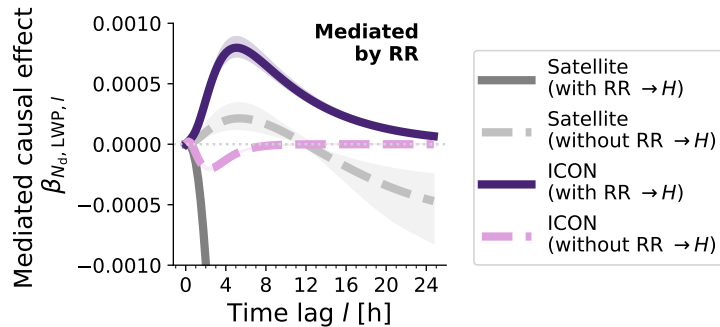
Supplementary Figure 6. Same as Fig. 8c but comparing the graph with the arrow from RR to H to the graph without this link
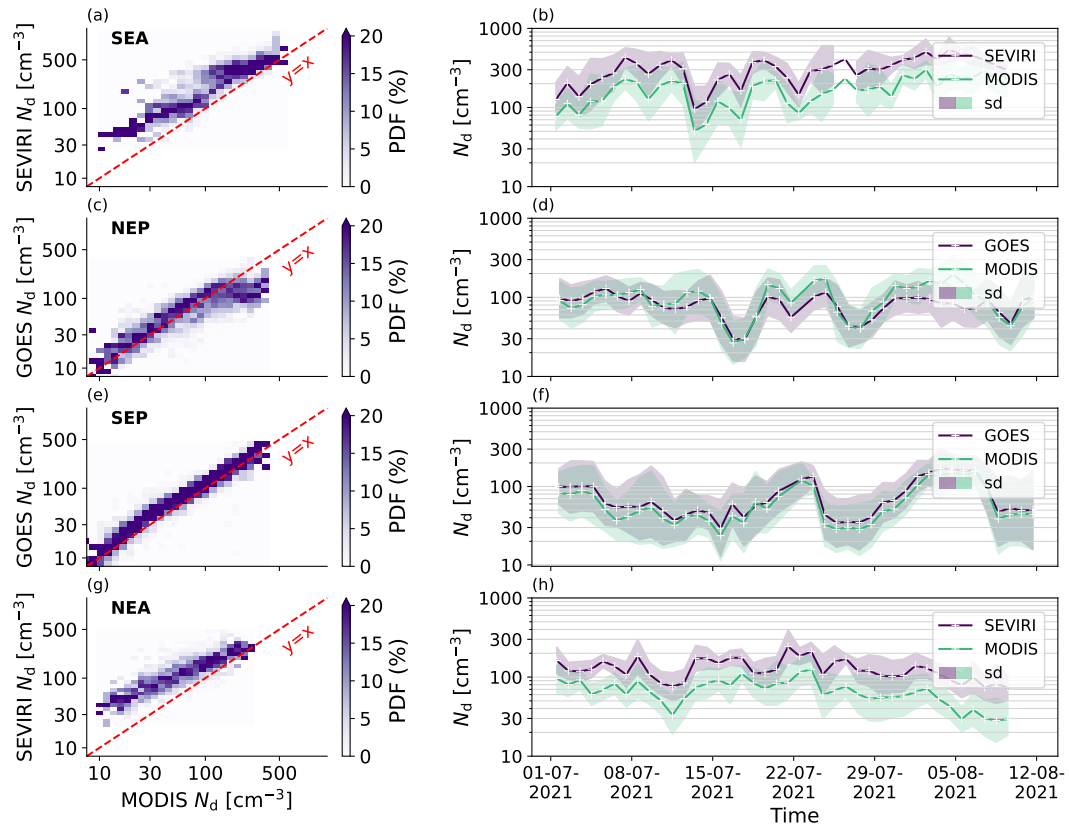
Supplementary Figure 7. N_d retrievals for MODIS Terra vs. geostationary satellites. **(a)**, **(c)**, **(e)**, **(g)** show 2D histograms of N_d from geostationary satellites as a function of N_d from MODIS for the four study regions. **(b)**, **(d)**, **(f)**, **(h)** show the same comparison, but as time series, averaged over the four regions.

References

Eastman, R., McCoy, I. L., Schulz, H., and Wood, R.: A Survey of Radiative and Physical Properties of North Atlantic Mesoscale Cloud Morphologies from Multiple Identification Methodologies, EGUsphere, pp. 1–33, https://doi.org/10.5194/egusphere-2023-2118, 2023.

McCoy, I. L., McCoy, D. T., Wood, R., Zuidema, P., and Bender, F. A.-M.: The Role of Mesoscale Cloud Morphology in the Shortwave Cloud Feedback, Geophysical Research Letters, 50, e2022GL101 042, https://doi.org/10.1029/2022GL101042, 2023.

Met Office: Cartopy: a cartographic python library with a Matplotlib interface, Exeter, Devon, https://scitools.org.uk/cartopy, 2010 - 2015.